Electronic and Optical Properties of Monolayer Hexagonal ZnSe from DFT Approach

Huda F. Salman, Shurooq S. Abed Al- Abbas

Department of Physics, College of Education for Pure Sciences, University of Babylon, Hilla, Iraq

Email: pure668.huda.fadel@student.uobabylon.edu.iq

Abstract

In this study, we have used the DFT approximation to investigate the electrical and optical characteristics of the hexagonal monolayer ZnSe compound. According to our calculations, ZnSe in a monolayer exhibits a Γ–M route symmetry transition, making it a direct band semiconductor. In excellent agreement with the experimental findings, the measured electronic band gap is around 2.66 eV. As a function of photon energy, the optical spectra of hexagonal ZnSe are measured in the x and z directions. With the majority of the optical response located along the x-axis, the absorption coefficient is highly anisotropic. The UV-Vis violet-blue spectrum's maximal absorption intensity is approximately 8×10^4 cm^{-1}. Our optical spectrum results made sense of the experimental findings.

Keywords: Zinc Selenide (ZnSe) monolayer, electronic properties, Optical properties,

1. Introduction

II-VI semiconductors have made great progress and are now widely used in optoelectronic fields due to their unique properties. Zinc sulfide (ZnS) is an n-type semiconductor with a bulk band gap that falls within the range of 3.5 to 3.7 eV. It demonstrates low levels of light absorption and a significantly elevated refractive index in the visible and infrared regions [1]. Moreover, ZnS possesses the ability to integrate different elements via doping, enabling it to serve as an n-type buffer layer for the creation of a heterojunction with p-type substances. Zinc selenide (ZnSe) is a semiconducting semiconductor belonging to the II-VI group. It has comparable physical characteristics to another substance. These qualities encompass a substantial energy difference of around 2.7 eV, a high coefficient for nonlinear optical phenomena, and little light absorption within the visible spectrum [2]**.** These materials could be used in optical waveguides, photovoltaic devices, blue-LEDs, blue lasing materials, photo detectors, solar cells, lasers, sensors, infrared windows, cathode ray tubes, electroluminescence, and catalytic applications [3–6]. Photonic devices often make use of II-VI semiconductors due to their optical characteristics, which are mainly linked to a straight band gap that falls within the right range [7]. Developing an optical device that functions in the infrared, red, green, and violet-blue spectrums is very challenging, yet essential for the advancement and commercialization of optical communication. Wider band gap semiconductors are necessary to maintain good quality. However, the presence of self-compensation phenomena poses challenges in producing stable layers on a substrate [8].

In order to develop optical devices that function at shorter wavelengths, a lot of work has been done on semiconductor materials from III-V (BN, GaN, GaAs, etc.) and II-VI (ZnO, ZnS, ZnSe, ZnTe, etc.) [9]. The high-density storage capacity of DVDs (digital video discs) can only be enhanced by the use of short-wavelength lasers. Electrochemical deposition [10], molecular beam epitaxy (MBE) [11], chemical vapour deposition (CVD) [12], stacked elemental layer deposition (SELD) [13], mechanical ball milling [14], and other methods are used to create the layer II–VI semiconductor materials. However, because of the agglomeration and cold-welding of the particles, mechanical ball milling is a primitive synthesis process that results in rough texture [15]. The addition of surfactants such as ZnCl2, ethanol, methanol, etc. has solved this issue [16].

Sharma et al. have successfully produced a ZnSe thin film at (298–393) K on a glass substrate using the condensation procedure. Using transmission measurements, they found that the optical gap dropped from 3.00 eV to 2.75 eV, the refractive

index increased from 2.38 to 2.48, and the ionicity increased from 0.446 to 0.425 when the substrate temperature climbed from 298 to 373 K [17]. ZnSe thin films prepared by chemical bath deposition (CBD) technique also exhibit a similar trend of decreased optical band gap from 3.5 eV to 3.0 eV when the temperature rises from 318 to 353 K. [18]. *Sun et al.* [19] successfully created a free-standing ZnSe monolayer with a direct band gap of 3.50 eV, which is necessary for the UV-range photocatalytic activity of water splitting. The photocurrent density is projected to be 8–200 times higher than that of bulk ZnSe and quantum dots, respectively. By using the RF sputtering thermal evaporation method to create a ZnSe thin film on Si-substrate, Mittal et al. [20] observed reduced loss of Rib waveguides at wavelengths between 2.5 μm and 3.7 μm. White light LEDs based on ZnSe were created, and they showed a 2 mW output power at 20 mA and a ~1000 h life period [21]. Following that, *Shirakawa* also created a white LED lamp based on II–VI (ZnSe) that has an optical output power of 4.3 mW, a forward voltage of 2.6 V, and a driving current of 20 mA [22]. Zincblende-wurtzite has undergone a phase change, as reported by *Zhang et al.* who used pulsed laser deposition to create nitrogen-doped ZnSe films [23].

2. Computational Methods

This work calculates the monolayer's electrical and optical properties using ab initio DFT computations in CASTEP software [24] using ultrasoft pseudopotentials and PBE exchange-correlation energy functional [25]. A Monkhorst-Pack grid (8x8x1) is used to discretize the first Brillouin zone (BZ). The optical properties were estimated using a 30x30x1 Monkhorst pack k-mesh, whereas the density of state (DOS) computations used a 16x16x1 mesh. In our numerical computations, we employ a kinetic energy cut-off of 510 eV for the plane-wave basis. The ZnSe monolayer structure exhibits complete atom relaxation, with forces and total energy converging at 0.01 eV/Å and 10^{-6} eV, respectively. To prevent cell layer contact, a 30Å vacuum space was used. The electron-electron interactions were treated by DFT-1/2 method considering the electron spin within Perdew-Burke-Ernzerhoff (PBE) parameterization [26]. The half-occupation state of Slater is incorporated into the corrective potential of the DFT approach, which is an effective way to correct the Kohn-Sham KS eigenvalues [27]. Because it uses semi-local functionals, this method is more credible for accurately estimating the band gap up to around 10.0 eV in a reasonable amount of time.

The electrical and optical properties are strongly related to the symmetrical structures of the ZnSe monolayer. Consequently, the initial step was to optimize the geometry of the ZnSe monolayer in its entirety. The fact that monolayer ZnSe has a hexagonal structure is well-known. The calculated values for the following parameters are in good agreement with previous investigations: the height between Zn and Se is 4.734 Å, the distance between Zn and Se is 4.098 Å, the bond between Zn and Se is 119.531 Å, the bond length between Zn and Se is 2.371 Å, the angle between Zn, Se and Zn is 119.531° is shown in Figure (1).

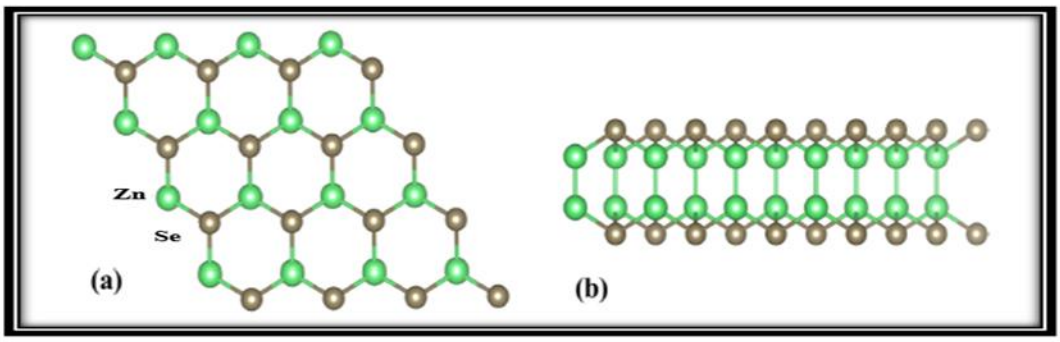

Figure .1. The geometric configuration of a ZnSe monolayer is depicted in (a) from a top perspective and (b) from a side view.

3- Result and Discussion

3.1 The electronic properties

ZnSe, in contrast to graphene, has a nonplanar structure with a hexagonal lattice and a dangling bond, δ (Å). The Force Field Approximation has been used to optimize the hexagonal structure, yielding an optimized lattice constant of a = b = 3.99 Å. The optimal lattice constant value agrees well with the previously calculated values of 4.10 Å [37] and 3.965 Å [36]. Also, the thermodynamical stability has been confirmed by calculating the phonon DOS and phonon band as shown in Fig. 2. Furthermore, the electronic and optical properties were performed for the relaxed system. A reducing in dimensionality from bulk to monolayer gives the quantum confinement effect which characterizes the band gap opening. This phenomenon has the direct impact on the optical properties of the system. The energy band gap in ZnSe can be determined by quantifying the energy variance among the lowermost point of the conduction band (CBM) and the uppermost point of the valence band (VBM). Figure 2 depicts the computed band structure of a solitary ZnSe layer. Evidently, this indicates the presence of a distinct energy gap directly at the Fermi level. The ZnSe monolayer is a semiconductor with a direct bandgap of 2.66 eV. The VBM is situated along the Γ–M trajectory, while the CBM is positioned at the M-point. These findings are consistent with the experimental results [27, 28].

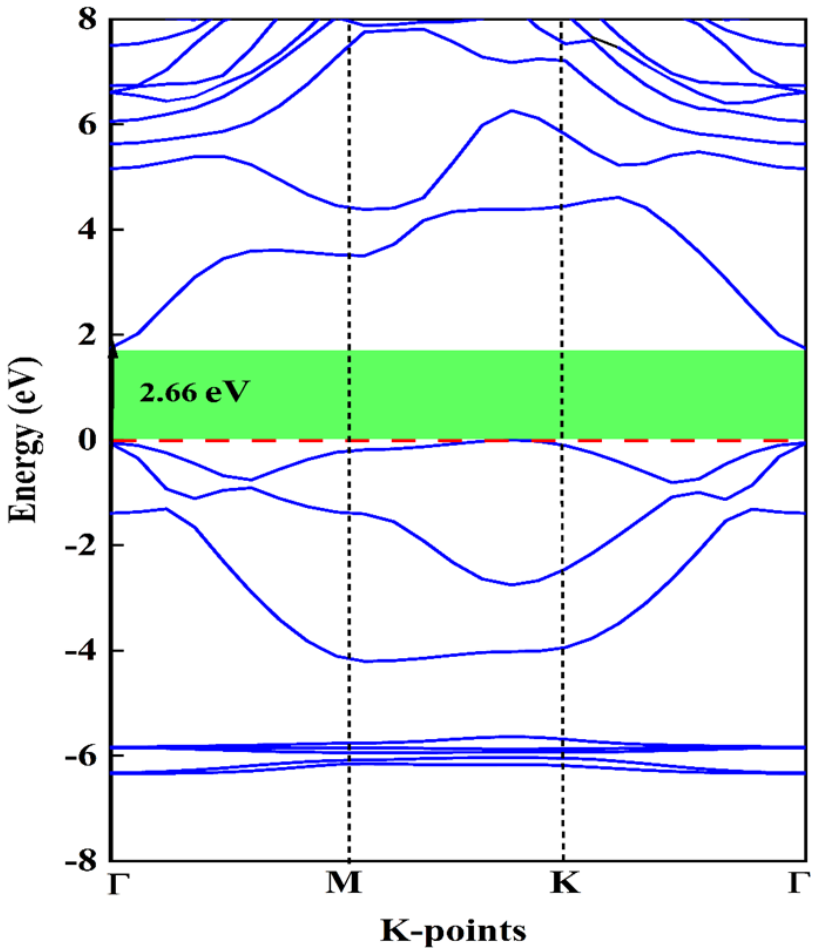

Figure .2. The calculated band structure of ZnSe monolayer.

Furthermore, we considered the overall and partial densities of states for a single layer of ZnSe, as depicted in Figure 3. Upon careful analysis of this image, it is apparent that there are three distinct structures in the density of electronic states, which are clearly divided by gaps. The primary contribution to the initial structure, which spans from -6.8 to -5.2 eV, comes from the 3*d*-Zn states,

with a little contribution from the 4s.3p-Zn and 4s.4p-Se states. The second structure displays an energy range spanning from -4.4 eV to -3.8 eV, which can be ascribed to the existence of 4s.4p.3d-Zn and 4p-Se. The states with energies ranging from -2.1 eV to the Fermi level are mostly affected by the 3d-3p states of Zn and the 4p levels of Se. The conduction band demonstrates the abundance of $s.p.d$ states throughout all atoms.

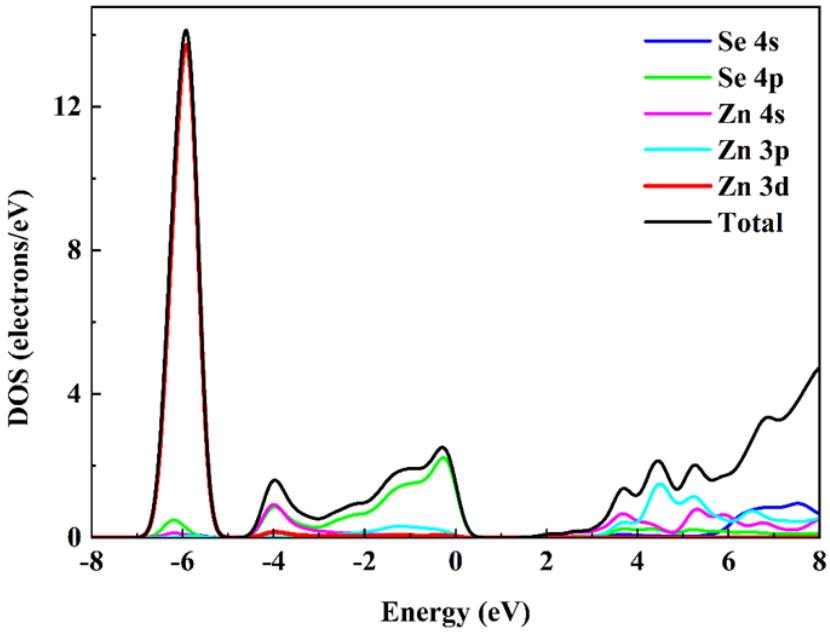

Figure. 3. The ZnSe density of states, both total and partial

3.2 The optical properties

The optical properties are the response of a material due to the interaction with the incident photon energy. The results of optical properties are shown as a function of photon energy in eV for both perpendicular and parallel axes (a) real and imaginary part of the dielectric function (b) Absorption coefficient (c) optical conductivity (d) loss function, (e) reflection and refractive index are presented in Fig. 6(a–d), respectively. The dielectric function of a material describes how the substance responds to electromagnetic radiation in terms of its linear spectrum. The real and imaginary part of complex quantity is expressed as in following equation [29]:

$$\varepsilon(\omega) = \varepsilon_1(\omega) + i\varepsilon_2(\omega) \quad (1)$$

where ε_1 real and ε_2 imaginary part of the dielectric function respectively. The real part of the dielectric function is obtained by the Kramers- Kronig transformation from its corresponding real and imaginary part as [29]:

$$\varepsilon_1(\omega) = 1 + \frac{2}{\pi}\, p \int_0^{\infty} \frac{\omega' \varepsilon_2(\omega')}{\omega'^2 - \omega^2} d\omega' \quad (2)$$

$$\varepsilon_2(\omega) = \frac{2e^2\pi}{\Omega\varepsilon_0} |\langle \psi_k^c | \hat{u} \times r | \psi_k^v \rangle| \, \delta(E_k^c - E_k^v - E) \quad (3)$$

The dielectric constant exhibits variations in response to the energy of the photon, as depicted in figure 4(a). A distinct maximum peak is found in both regions of the insulator constant. The maximum value of the actual dielectric function occurs at 6 eV, while the imaginary dielectric function reaches its top at 7 eV. Subsequently, it progressively decreases and converges towards a stable magnitude as the photon energy increases along the x-axis. This is due to the arrangement of Zn and Se atoms on a single plane, which restricts their interaction. This is accomplished by generating a state of emptiness or absence of matter along the z-axis. Hence, the polarizability is substantially smaller than the x-direction polarizability. The lower ε_1 spectra along the z-axis, which primarily occur along the x-axis, prove that the substantial is aggressively intermingling with the input photon in the energy

range of (4. -15 eV). This observation is consistent with the acquired results [30].

The absorption coefficient was calculated from the following equation [31]

$$\alpha\ (\omega) = \frac{\sqrt{2}\omega}{c}\left(\sqrt{\varepsilon_1^2(\omega) + \varepsilon_2^2(\omega)} - \varepsilon_1(\omega)\right)^{\frac{1}{2}} \quad (4)$$

Figure 4(b) demonstrates that there is an absorption coefficient of light within the energy range of 7 to 12 eV. ZnSe monolayer has optical absorption mostly in the ultraviolet spectrum, with two notable peaks observed at energy levels of 7.8 and 11.3 eV. As a result, this monolayer possesses the capacity to absorb ultraviolet (UV) radiation. The observed peaks arise from the electron conversion occurring between occupied S-p and sp^2-p orbitals to the unoccupied conduction band. The conclusions we have drawn are consistent with the outcomes documented in reference [30]. The effective absorption range of the ZnSe monolayer extends from 7 to 12 eV, covering the two prominent peaks observed in the Violet-Blue region of the UV spectra. The ZnSe monolayer shows great potential for use in optoelectronic and photoelectric devices, especially in the ultraviolet (UV) spectrum. Conversely, the absorption coefficients of a ZnSe monolayer closely mirror those of perovskite solar cells, as its value can exceed $8*10^5$ cm^{-1}.

The optical conductivity was calculated from relation [31]:

$$\sigma(\omega) = \frac{\omega}{4\pi}\varepsilon_2(\omega) \quad (5)$$

The optical conductivity of a ZnSe monolayer is depicted in Figure 4(c) as a function of photon energy. Thoroughly analyzing the Figure confirmed that this monolayer has semiconducting characteristics, as seen by the optical conductivity peak aligning with the band gap. Moreover, there is a clearly noticeable optical peak found at 7.8 eV. The emergence of this peak is a result of the interface among photons and electrons, with the maximum optical conductivity occurring inside the ultraviolet (UV) range. The ZnSe monolayer shows significant promise as a feasible choice for use in UV detectors.

The loss function was calculated from relation [31]:

$$L\ (\omega) = \frac{\varepsilon_2\ (\omega)}{\varepsilon_1^2(\omega) + \varepsilon_2^2(\omega)} \quad (6)$$

A representation of the loss function of photon energy can be seen in Figure 4(d). It is clear that the ZnSe monolayer exhibits two distinct peaks, one at 8.5 eV and the other at 11.6 eV. It is the plasma frequency that serves as the dividing line between the behavior of the material as a dielectric and as a metal. The loss of energy peaks shows the plasma frequency. To be more specific, any material can act as a dielectric at frequencies that are lower than the plasma frequency, and it will perform as a metal at frequencies that are greater than the plasma frequency. In accordance with what was mentioned before, the ultraviolet (UV) area is where the loss function is discovered to have its highest possible value.

The reflectivity was calculated from relation [32]:

$$R\ (\omega) = \frac{[n(\omega)-1]^2 + K^2(\omega)}{[n(\omega)+1]^2 + K^2(w)} \quad (7)$$

Figure 5(e) depicts the correlation between reflectivity and photon energy. An observation reveals that the reflectance at zero frequency is 0.9%. The reflectivity ratings reach a maximum of 88.7% and 76.92%. The ZnSe monolayer demonstrates its highest reflectivity in the ultraviolet (UV) range at energies of 8 and 11.3 eV, which corresponds to the absorption coefficient.

The refractive index was calculated from relation [32]:

$$n\ (\omega) = \frac{1}{\sqrt{2}}\left(\sqrt{\varepsilon_1^2(\omega) + \varepsilon_2^2(\omega)} + \varepsilon_1^2(\omega)\right)^{\frac{1}{2}} \quad (8)$$

Figure 5(f) depicts the correlation between the refractive index of a ZnSe monolayer and the photon's energy. The static index of refractive is 1.2. Nevertheless, the maximum attainable value of the index of refractive is 1.4 when the wavelength is 6.3 electron volts. After reaching this threshold, the index of refractive gradually decreases as the energy of photons increases. The drop continues until it achieves a steady state at a fixed value of 0.9 when the photon energy hits 17.5 eV. When the phase velocity of the electromagnetic wave exceeds the speed of light (v_p > c), the number of spectra decreases to fewer than 1 for values below 17.5. This phenomenon is considered unphysical. Moreover, this occurrence happens near the point where the

material absorbs the most energy due to the oscillation of its plasmonic vibrations. The plasmonic frequency is measured to be 3.14 (eV), whereas the threshold plasmonic frequency is calculated to be $\omega_p = 2.53 \times 10^4$ (cm^{-1}), which corresponds to the obtained result [33].

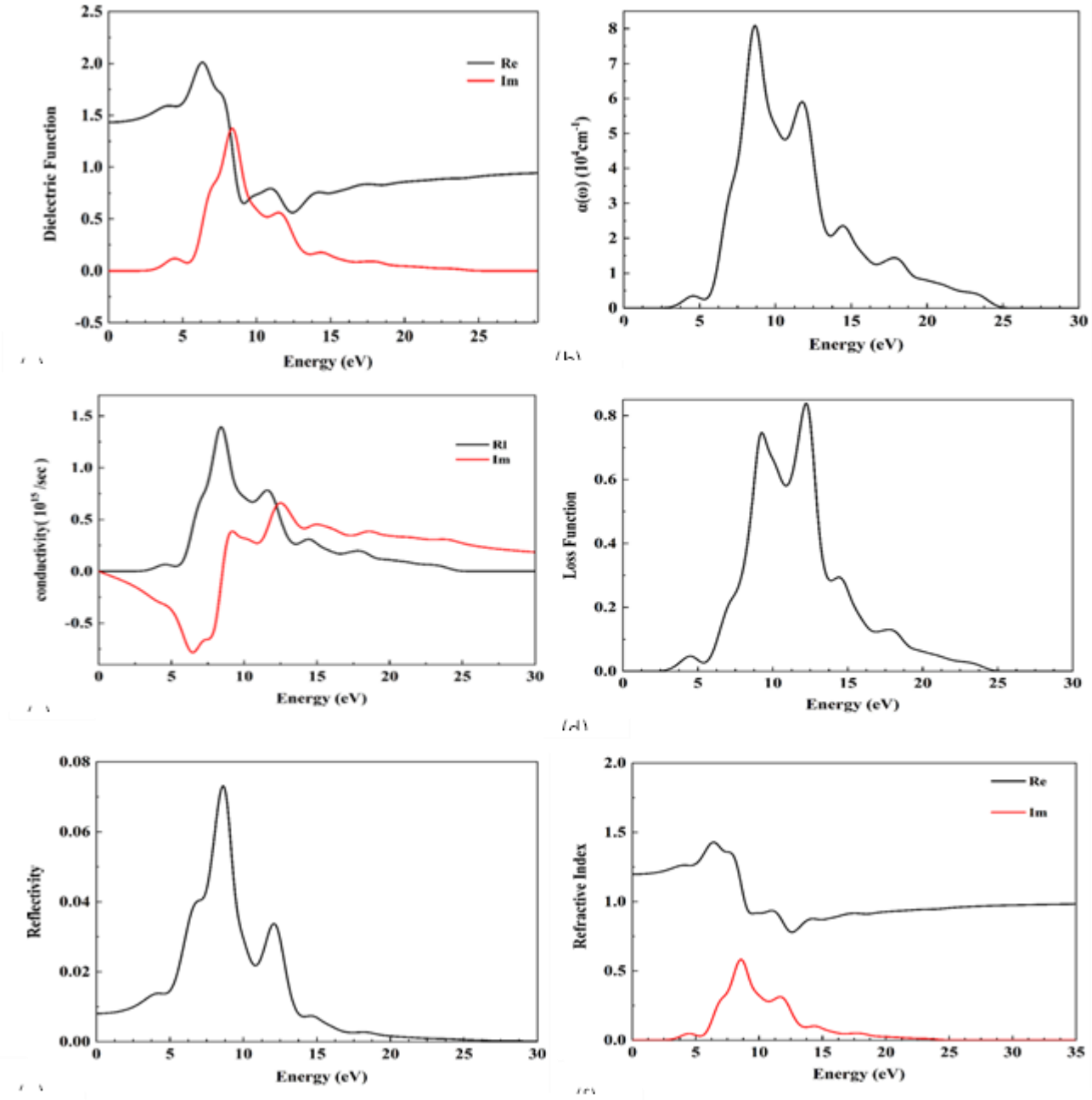

Figure. 4. Optical properties of ZnSe (a) dielectric function (b) Absorption coefficient, (c) optical conductivity and (d) loss function (e) reflectivity and (f) Refractive index.

4- **Conclusion**

In conclusion, we have examined the electrical, magnetic, and optical properties of the monolayer hexagonal ZnSe combination using the density functional theory (DFT) approximation. By adding Slater's half-occupation state to the Kohn-Sham KS eigenvalue correction, DFT is a new type of semi-local correlation functional. Consequently, it offers a rapid and useful method for estimating the

semiconducting band gap up to around 10 eV. According to our computation, monolayer ZnSe exhibits a transition along the Γ–M route symmetry, making it a direct band semiconductor. The electronic band gap measured value is ~2.66 eV, which is in excellent accord with the experimental findings. The x- and z-axes are used to measure the hexagonal ZnSe optical spectra in relation to photon energy. The bulk of the optical response is located along the x-axis, and the absorption coefficient is very anisotropic. Approximately 8×10^4 cm^{-1} is the greatest absorption strength in the violet-blue area of the UV–Vis. spectrum. Our optical spectrum results made sense of the experimental findings.

References

[1] Y. Zhang X. Y. Dang, J. Jin, T. Yu, B. Z. Li, Q. He and Y. Sun,, "ZnS thin film deposited with chemical bath deposition process directed by different stirring speeds," *Appl. Surf. Sci.*, vol. 256, no. 22, pp. 6871–6875, 2010.

[2] P. Chelvanathan,Y. Yusoff, F. Haque, M. Akhtaruzzaman, M. M. Alam, Z. A. and N. Amin, "Growth and characterization of RF-sputtered ZnS thin film deposited at various substrate temperatures for photovoltaic application," *Appl. Surf. Sci.*, vol. 334, pp. 138–144, 2015.

[3] R. Khenata, A. Bouhemadou, M. Sahnoun, A. H. Reshak, H. Baltache, and M. Rabah, "Elastic, electronic and optical properties of ZnS, ZnSe and ZnTe under pressure," *Comput. Mater. Sci.*, vol. 38, no. 1, pp. 29–38, 2006.

[4] S. Wei, J. Lu, and Y. Qian, "Density Functional Study of 2D Semiconductor CdSe· hda 0.5 (hda= 1, 6-hexanediamine) and Its Excitonic Optical Properties," *Chem. Mater.*, vol. 20, no. 23, pp. 7220–7227, 2008.

[5] R. A. Casali and N. E. Christensen, "Elastic constants and deformation potentials of ZnS and ZnSe under pressure," *Solid State Commun.*, vol. 108, no. 10, pp. 793–798, 1998.

[6] J. Sörgel and U. Scherz, "Ab initio calculation of elastic constants and electronic properties of ZnSe and ZnTe under uniaxial strain," *Eur. Phys. J. B-Condensed Matter Complex Syst.*, vol. 5, pp. 45–52, 1998.

[7] V. A. Gnatyuk, "Photoconductivity of ZnSe crystals under high excitation rates," *Semicond. Sci. Technol.*, vol. 15, no. 6, p. 523, 2000.

[8] A. Janotti and C. G. Van de Walle, "Fundamentals of zinc oxide as a semiconductor," *Reports Prog. Phys.*, vol. 72, no. 12, p. 126501, 2009.

[9] S. K. Tripathy and A. Pattanaik, "Optical and electronic properties of some semiconductors from energy gaps," *Opt. Mater. (Amst).*, vol. 53, pp. 123–133, 2016.

[10] P. Ilanchezhiyan, G.M. Kumar, X. Fu, S. Poongothai, T.W. Kang, Ultrasonic-assisted synthesis of ZnTe nanostructures and their structural, electrochemical and photoelectrical properties, Ultrason. Sonochem. 39 (2017) 414–419.

[11]X. Li, B. Wei, J. Wang, X. Li, H. Zhai, J. Yang, Synthesis and comparison of the photocatalytic activities of ZnSe(en)0.5, ZnSe and ZnO nanosheets, J. Alloys Compd. 689 (2016) 287–295

[12] E. Krause, H. Hartmann, J. Menninger, A. Hoffmann, Ch Fricke, R. Heitz, B. Lummer, V. Kutzer, I. Broser, Influence of growth non-stoichiometry on optical properties of doped and non-doped ZnSe grown by chemical vapour deposition, J. Crys. Growth 138 (1994) 75–80.

[13] L.R. Curz, R.R. de Avillez, The formation of CdTe thin films by the stacked elemental layer method, Thin Solid Films 373 (2000) 15–18.

14]C. Suryanarayana, E. Ivanov, Mechanochemical synthesis of nanocrystalline metal powders, in: Advances in Powder Metallurgy Properties, Processing and Applications, Woodhead Publishing Series in Metals and Surface Engineering, 2013 ,pp. 42–68.

[15] M. Achimovicova, Z. Bujnakova, M. Fabian, A. Zorkovoska, Study of deaggregation of mechanochemically synthesized ZnSe nanoparticles by re-milling in the presence of ZnCl2 solution, Acta Montanistica Slovaca Rocnik 18(2013) 119.124–

[16] J. Sharma, H. Singh, T. Singh, A. Thakur, Structural, optical and photo-electrical properties of nanocrystalline ZnSe thin films, J. Mater. Sci: Mater. Electron. 29–5688 (2018) .5695

[17] C. Mehta, G.S.S. Saini, J.M. Abbas, S.K. Tripathi, Effect of deposition parameters on structural, optical and electrical properties of nanocrystalline ZnSe thin films, Appl. Surf. Sci. 256 (2009) 608–614.

[18] Y.F. Sun, Z.H. Sun, S. Gao, H. Cheng, Q.H. Liu, J.Y. Piao, T. Yao, C.Z. Wu, S.L. Hu, S.Q. Wei, Y. Xie, Fabrication of flexible and freestanding zinc chalcogenide single layers, Nat. Commun. 3 (2012) 1057.

[19] C.J. Tong, H. Zhang, Y.N. Zhang, H. Liu, L.M. Liu, New manifold two-dimensional single-layer structures of zinc-blende compounds, J. Mater. Chem. 2 (2014) 17971.

[20] V. Mittal, N.P. Sessions, J.S. Wilkinson, G.S. Murugan, Optical quality ZnSe films and low loss waveguides on Si substrates for mid-infrared applications, Opt. Mat. Exp. 7 (2017) 717.

[21] K. Katayama, H. Matsubara, F. Nakanishi, T. Nakamura, H. Doi, A. Saegusa, T. Mitsui, T. Matsuoka, M. Irikura, T. Takebe, S. Nishine, T. Shirakawa, ZnSe-based white LEDs, J. Cryst. Growth 214–215 (2000) 1064–1070.

[22] T. Shirakawa, Effect of defects on the degradation of ZnSe-based white LEDs, Mat. Sci. Eng. B91–92 (2002) 470–475.

[23] X. Zhang, D. Wang, M. Beres, L. Liu, Z. Ma, P. Yu, S. Mao, Zincblende-wurtzite phase transformation of ZnSe films by pulsed laser deposition with nitrogen doping, Appl. Phys. Lett. 103 (2013), 082111.

[24] J. P. Perdew, K. Burke, and M. Ernzerhof, "Generalized gradient approximation made simple," *Phys. Rev. Lett.*, vol. 77, no. 18, p. 3865, 1996.

[25] D. P. Rai, A. Laref, M. Khuili, S. Al-Qaisi, T. V Vu, and D. D. Vo, "Electronic, magnetic and optical properties of monolayer (ML) hexagonal ZnSe on vacancy defects at Zn sites from DFT-1/2 approach," *Vacuum*, vol. 182, p. 109597, 2020.

[26] J.P. Perdew, K. Burke, M. Ernzerhof, Generalized gradient approximation made simple, Phys. Rev. Lett. 77 (1996), 3868-3865.

[27] L.G. Ferreira, M. Marques, L.K. Teles, Approximation to density functional theory for the calculation of band gaps of semiconductors, Phys. Rev. B 78 (2008) 125116.

[28] M.S. Khan, L. Shi, Impact of vacancy defects on optoelectronic and magnetic properties of Mn-doped ZnSe, Comp. Mater. Sci. 174 (2020) 10949.

[29] M. Safari, Z. Izadi, J. Jalilian, I. Ahmad, S.J. Asadabadi, Metal mono-chalcogenides ZnX and CdX (X=S, Se and Te) monolayers: chemical bond and optical interband transitions by first principles calculations, Phys. Lett. 381 (2017) 663–670, https://doi.org/10.1016/j.physleta.2016.11.040.

[30] L. G. Valluzzi, M. G. Valluzzi, G. N. Darriba, M. Meyer, and L. C. Damonte, "Surfactant and dopant addition effect on optical and structural properties of ZnSe (Te) nanostructured semiconductors," *J. Alloys Compd.*, vol. 829, p. 154488, 2020.

[31] S. S. A. Al-Abbas, M. K. Muhsin, and H. R. Jappor, "Tunable optical and electronic properties of gallium telluride monolayer for photovoltaic absorbers and ultraviolet detectors," *Chem. Phys. Lett.*, vol. 713, pp. 46–51, 2018.

[32] G. Falah, I. Witwit, and S. S. A. Al-abbas, "Adsorption of Gas Molecules on HfSSe Janus Monolayer," vol. 20, no. 1, pp. 150–161, 2022, doi: 10.14704/nq.2022.20.1.NQ22069.

[33] L. G. Valluzzi, M. G. Valluzzi, G. N. Darriba, M. Meyer, and L. C. Damonte, "Surfactant and dopant addition effect on optical and structural properties of ZnSe (Te) nanostructured semiconductors," *J. Alloys Compd.*, vol. 829, p. 154488, 2020.